jove

Mechanostimulation of Multicellular Organisms Through a High-Throughput Microfluidic Compression System

Utku M. Sönmez[1], **Nolan Frey**[2], **Jonathan S. Minden**[2], **Philip R. LeDuc**[1]

[1] Department of Mechanical Engineering, Carnegie Mellon University [2] Department of Biological Sciences, Carnegie Mellon University

Corresponding Authors

Jonathan S. Minden
minden@andrew.cmu.edu

Philip R. LeDuc
prl@andrew.cmu.edu

Citation

Sönmez, U.M., Frey, N., Minden, J.S., LeDuc, P.R. Mechanostimulation of Multicellular Organisms Through a High-Throughput Microfluidic Compression System. *J. Vis. Exp.* (190), e64281, doi:10.3791/64281 (2022).

Date Published

December 23, 2022

DOI

10.3791/64281

URL

jove.com/video/64281

Abstract

During embryogenesis, coordinated cell movement generates mechanical forces that regulate gene expression and activity. To study this process, tools such as aspiration or coverslip compression have been used to mechanically stimulate whole embryos. These approaches limit experimental design as they are imprecise, require manual handling, and can process only a couple of embryos simultaneously. Microfluidic systems have great potential for automating such experimental tasks while increasing throughput and precision. This article describes a microfluidic system developed to precisely compress whole *Drosophila melanogaster* (fruit fly) embryos. This system features microchannels with pneumatically actuated deformable sidewalls and enables embryo alignment, immobilization, compression, and post-stimulation collection. By parallelizing these microchannels into seven lanes, steady or dynamic compression patterns can be applied to hundreds of *Drosophila* embryos simultaneously. Fabricating this system on a glass coverslip facilitates the simultaneous mechanical stimulation and imaging of samples with high-resolution microscopes. Moreover, the utilization of biocompatible materials, like PDMS, and the ability to flow fluid through the system make this device capable of long-term experiments with media-dependent samples. This approach also eliminates the requirement for manual mounting which mechanically stresses samples. Furthermore, the ability to quickly collect samples from the microchannels enables post-stimulation analyses, including -omics assays which require large sample numbers unattainable using traditional mechanical stimulation approaches. The geometry of this system is readily scalable to different biological systems, enabling numerous fields to benefit from the functional features described herein including high sample throughput, mechanical stimulation or immobilization, and automated alignment.

Introduction

Living systems constantly experience and respond to various mechanical inputs throughout their lifetimes[1]. Mechanotransduction has been linked to many diseases, including developmental disorders, muscle and bone loss, and neuropathologies through signaling pathways directly or indirectly affected by the mechanical environment[2]. However, the genes and proteins that are regulated by mechanical stimulation[3] in the mechanosensitive signaling pathways[4] remain largely unknown[5], preventing the elucidation of the mechanical regulation mechanisms and the identification of molecular targets for diseases associated with pathological mechanotransduction[6,7]. One limiting factor in projecting mechanobiology studies onto the related physiological processes is using individual cells with conventional culture dishes instead of intact multicellular organisms. Model organisms, such as *Drosophila melanogaster* (fruit fly), have contributed greatly to understanding the genes, signaling pathways, and proteins involved in animal development[8,9,10]. Nevertheless, using *Drosophila* and other multicellular model organisms in mechanobiology research has been hindered by challenges with experimental tools. Conventional techniques for preparing, sorting, imaging, or applying various stimuli require mostly manual manipulation; these approaches are time-consuming, require expertise, introduce variability, and limit the experimental design and sample size[11]. Recent microtechnological advancements are a great resource for enabling novel biological assays with very high throughput and highly controlled experimental parameters[12,13,14].

This article describes the development of an enhanced microfluidic device to align, immobilize, and precisely apply mechanical stimulation in the form of uniaxial compression to hundreds of whole *Drosophila* embryos[15] (**Figure 1**). Integration of the microfluidic system with a glass coverslip allowed high-resolution confocal imaging of the samples during the stimulation. The microfluidic device also enabled fast collection of the embryos after the stimulation for running -omics assays (**Figure 2**). Explanations of the design considerations of this device, as well as the fabrication using soft lithography and experimental characterization, are described herein. Since making a silicon wafer mold of such a device requires a uniform coating of thick photoresist (thickness >200 µm) over large areas with high aspect ratio (AR) trenches (AR >5), this method considerably modified the traditional photolithographic mold fabrication protocol. In this way, this method facilitated the handling, adhesion, coating, patterning, and development of the photoresist. Additionally, potential pitfalls and their solutions are discussed. Lastly, the versatility of this design and fabrication strategy was demonstrated using other multicellular systems such as *Drosophila* egg chambers and brain organoids[16].

Protocol

1. Preparation of the silicon wafer mold

1. Clean the silicon wafer (see **Table of Materials**) first with acetone and then with isopropyl alcohol (IPA).
2. Place the silicon wafer on a 250 °C hot plate for 30 min for dehydration bake (**Figure 3A**).
3. Coat the silicon wafer with hexamethyldisilazane (HDMS) in a vapor prime oven (see **Table of Materials**) (process temperature: 150 °C, process pressure: 2 Torr, process time: 5 min, HDMS volume: 5 µL) (**Figure 3B**).
4. Place a bottle of SU-8 2100 photoresist (see **Table of Materials**) in a 60 °C oven for 15 min to reduce its viscosity.

   NOTE: Upon heating in the oven, the viscosity of the photoresist decreases. Photoresists with lowered

viscosity can be handled more easily and can be poured more accurately on top of the wafer.

5. Place the silicon wafer on a 60 °C hot plate and pour 1 mL of the heated photoresist for each inch of the wafer until the photoresist covers most of the surface (**Figure 3C**).
6. Transfer the photoresist-coated silicon wafer to a spin coater (see **Table of Materials**).
7. Apply pre-spin first at 250 rpm for 30 s and then at 350 rpm for another 30 s, both with 100 rpm/s acceleration (**Figure 3D**).
8. Remove the excess photoresist from the edges of the silicon wafer using a cleanroom swab.
9. Apply a spin first at 500 rpm for 15 s with 100 rpm/s acceleration and then at 1450 rpm for 30 s with 300 rpm/s acceleration (**Figure 3E**).
10. Remove the edge bead with a cleanroom swab.
11. Place the silicon wafer on a 50 °C hot plate and spray acetone on the wafer to remove imperfections and promote uniform coating (**Figure 3F**).
12. Slowly ramp up the temperature of the hot plate to 95 °C at the rate of 2°C/min.
13. Soft bake the silicon wafer at 95 °C for 50 min (**Figure 3G**).
14. Slowly cool down the hot plate to room temperature at a rate of 2°C/min.
15. Place the silicon wafer on a mask aligner (see **Table of Materials**) and place the photomask on top of it (please refer to **Supplementary Figure 1** for the photomask geometry).
16. Expose the silicon wafer to 350 mJ/cm^2 UV light (35 mW/cm^2 for 10 s) through the photomask using the contact mask aligner (**Figure 3H**).
17. Apply consecutive post-exposure bakes on the silicon wafer by placing the wafer on a hot plate at 50 °C for 5 min, at 65 °C for an additional 5 min, and finally at 80 °C for another 20 min (**Figure 3I**).
18. Slowly cool down the silicon wafer to room temperature at the rate of 2 °C/min.
19. Place a magnetic stirrer with a slightly smaller diameter than the silicon wafer in a beaker. Turn the silicon wafer upside-down and place it on top of the beaker.
20. Place the beaker inside another larger beaker and fill the larger beaker with a fresh developer solution (see **Table of Materials**). Leave the silicon wafer submerged in the developer for 30 min with the stirrer turned on (**Figure 3J**).
21. Transfer the silicon wafer into an ultrasonic bath sonicator filled with the fresh developer for 1 h at 40 kHz (**Figure 3K**).
22. Thoroughly wash the silicon wafer with an IPA solution to obtain the final silicon wafer mold (**Figure 3L**).

2. Fabrication of the microfluidic chip

1. Place the silicon wafer mold in a desiccator together with 10 drops (~500 µL) of Trichloro(1H,1H,2H,2H-perfluorooctyl)silane (PFOCTS, see **Table of Materials**) in a small weigh boat nearby.
2. Connect the desiccator to a vacuum pump at approximately 200 Torr for 30 min.
3. Turn off the desiccator valve and disconnect the vacuum pump overnight for PFOCTS coating.

4. Prepare the pre-cured polydimethylsiloxane (PDMS) solution by mixing the PDMS base with the curing agent (see **Table of Materials**) at a 10:1 ratio.
5. Degas the mixture by placing it into a centrifuge (500 x *g* for 5 min at room temperature).
   NOTE: This centrifugation allows bubbles to migrate to the top surface and consequently be removed in a short period of time.
6. Pour the degassed PDMS solution onto the silicon wafer mold.
7. Degas it again to remove the air bubbles trapped on the mold surface.
8. Cure the PDMS in a 60 °C oven for 1 h and 50 min (**Figure 3M**).
9. Use a scalpel to cut the borders of the cured PDMS region corresponding to the microfluidic chip geometry (**Figure 3N**).
10. Peel the PDMS part and place it upside-down on a cutting mat.
11. Use a razor to cut the PDMS part into its final shape (**Figure 3O**).
12. Punch the inlet and outlet holes on PDMS using a biopsy punch (see **Table of Materials**) or a needle with a blunt tip (**Figure 3P**).
    1. For the embryo inlet hole, use a 4 mm diameter punch.
    2. For the embryo outlet holes, use a 1.3 mm diameter punch.
    3. For the gas inlet hole, use a 2 mm punch.
13. Use a piece of scotch tape to remove any particulate that might remain on the patterned surface of the PDMS.
14. Clean a 24 mm x 60 mm rectangular glass slide first with acetone and then with IPA.
15. Dry the glass surface with an air gun connected to a filtered air source.
16. Apply a dehydration bake to the glass slide by placing it on a 250 °C hot plate for 2 h (**Figure 3Q**).
17. Cover the glass slide with a beaker to prevent surface contamination.
18. Place the PDMS, with its patterned side up, and the dehydrated glass slide into a plasma cleaner (see **Table of Materials**).
19. Treat the PDMS and the glass slide with oxygen plasma at 18 W for 30 s.
20. Place the PDMS on the glass slide with its patterned surface facing toward the glass slide to seal the microchannels *via* covalent bonding (**Figure 3R**).
21. Use tweezers to gently push the PDMS part against the glass slide to ensure full conformational contact.
22. Store the completed microfluidic chip at room temperature overnight to allow the bonding to reach its final strength.

3. Preparation of the fruit fly embryos

1. Allow Oregon-R adult flies to lay eggs on apple juice agar plates (1.5% agar, 25% apple juice, 2.5% sucrose) and collect the plates at the desired developmental time after egg laying for the given experiment.
   NOTE: For the present experiments, the plates were collected at 140 min to prepare and sort for embryos at the cellularization stage[17].

2. Flood the agar with embryo egg wash (0.12 M NaCl, 0.04% Triton-X 100) and gently agitate the embryos with a paintbrush to dislodge them from the agar.
3. Transfer the embryos to a 50% bleach solution for 90 s, stirring occasionally. Strain the embryos through a tissue sieve and thoroughly wash away the bleach solution with water.
4. Transfer the embryos to a 90 mm glass Petri dish with enough embryo egg wash to fully cover the embryos.
5. Examine the embryos with transillumination on a dissecting microscope and select embryos of the desired development stage for loading into the microfluidic device.
   NOTE: In this application, embryos at the cellularization stage were selected. The detailed descriptions of how to ensure proper developmental stage selection can be found in the laboratory handbook for *Drosophila*[17].

4. Applying mechanical stimulation to fruit fly embryos using the microfluidic chip

1. Prime all seven embryo microchannels by filling them with 0.4 µm filtered IPA through the main embryo inlet port.
2. Replace the IPA with 0.4 µm filtered deionized (DI) water.
3. Replace the DI water with embryo egg wash solution.
4. Collect approximately 100 preselected embryos from the glass Petri dish using a glass pipette.
5. Pipette the embryos into the embryo inlet port (**Figure 4A**).
6. Apply an approximately 3 PSI negative pressure (i.e., vacuum) to the gas inlet using a portable vacuum pump to open up the embryo microchannels.
7. Tilt the microfluidic chip downward for the embryos to automatically align and settle into the embryo microchannels (**Figure 4B**).
8. If the embryo microchannel inlets get clogged by multiple embryos entering simultaneously, tilt the microfluidic chip upward and then downward again to clear the clogging.
9. Based on the required throughput, introduce as many as 300 embryos into the embryo microchannels.
10. Once the embryo loading is completed, remove the vacuum to immobilize the embryos.
11. Tilt the microfluidic chip back to the horizontal position (**Figure 4C**).
12. Connect a portable positive pressure source (see **Table of Materials**) with a pressure gauge to the gas inlet to apply 3 PSI compression (**Figure 4D**).
13. Continuously check the pressure gauge to ensure a consistent compression level is applied.
14. If live imaging experiments will be conducted on the mechanically stimulated embryos, place the microfluidic chip on a standard microscope stage glass slide holder with the gas inlet connected to the pressure source.
15. Once the compression experiment is completed, the embryos can be collected for downstream analysis. In order to do this, first, apply the vacuum to the gas inlet to free the embryos.
16. Then, tilt the microfluidic chip upward for the embryos to move toward the embryo introduction port (**Figure 4E**).
17. Collect the embryos from the microfluidic chip using a glass pipette.
    NOTE: Upon collection, the effects of compression on embryonic development and viability can be investigated by growing the fruit flies into adulthood. The high-

throughput processing capability of the microfluidic device also enables embryos to be used in downstream omics-based assays that require a large number of samples (**Figure 2**).

Representative Results

The microfluidic system is divided into two sub-compartments separated by deformable PDMS sidewalls. The first compartment is the liquid system where *Drosophila* embryos are introduced, automatically aligned, lined up, and compressed. The second compartment is a gas system where the gas pressure at either side of the compression channels is controlled *via* dead-end microchannels to precisely control the effective width of the compression channels. The microfluidic device is sealed with a glass slide at the bottom, which enables high-resolution live imaging of the samples (**Supplementary Figure 2**) for the relevant dimensions of the microfluidic device.

Multicellular organisms such as *Drosophila* embryos are selected at the desired embryonic developmental stage. In the case of the *Drosophila* embryos, all the developmental stages are equally compatible with this approach since the embryo size does not change until they hatch. Selected samples are introduced into the microfluidic device through the large inlet (i.e., 4 mm diameter) using a glass micropipette. The device is then tilted downward to allow the embryos to flow into the seven compression channels organized in a parallel fashion. The narrowing atrium that connects the embryo inlet to the compression channel ensures automatic alignment of the embryos before they reach the entrance of the compression channels. The vacuum applied to the gas inlet deflects the deformable sidewalls outward, increasing the effective microchannel width and allowing the embryos to enter the compression channels sequentially. The seven compression channels are 22 mm long and, in parallel, can accommodate up to 300 *Drosophila* embryos in a single run. Compression channels terminate in a bottleneck where the width of the microchannel decreases to a level much smaller than that of the samples, which allows fluid to flow through while retaining the embryos. Through this approach, the embryos are concentrated within the compression channels. After the introduction of the embryos, the vacuum in the gas inlet is removed, and the microchannel sidewalls return to their original position and immobilize the lined-up embryos from either side. Compression can be achieved by applying positive pressure to the gas inlet, which deflects the deformable sidewalls inward and reduces the effective microchannel width. The amount of compression applied to embryos can be precisely regulated by tailoring the microchannel dimensions, the thickness of the deformable sidewalls, the Young's Modulus of the PDMS, and the applied pressure. After the compression experiment, the embryos can be collected for downstream analysis by applying a vacuum to the gas inlet and tilting the microfluidic device in another direction.

This microfluidic device was fabricated using soft lithography[18]. However, fabricating thick structures with high aspect ratio features using ultrathick photoresist requires major deviations from protocols defined for the standard fabrication (**Figure 3**). Along with hexamethyldisilazane (HDMS) coating, the silicon wafers were cleaned before spin coating to remove organic residues and baked to remove surface moisture. These extra steps enhanced the bonding of the thick photoresist layer to the silicon wafer. The photoresist was also heated before pouring to decrease viscosity, which was crucial for covering the entire wafer surface. The target photoresist coating thickness was achieved through three spinning steps, where each spinning step gradually removed

excess photoresist without contaminating the wafer surface. Inspired by previously published methods[19], acetone was sprayed, which is one of the solvents of the photoresist, on the silicon wafer to eliminate photoresist imperfections and increase the uniformity of the coating. During the consecutive baking steps, the temperature was changed slowly to minimize thermal stress, which could lead to the delamination of the photoresist from the silicon wafer. Due to similar concerns, the baking temperature was decreased while increasing its duration. One of the most challenging steps in the photolithographic fabrication of high aspect ratio trenches was the removal of the uncured photoresist after UV exposure. To maximize the developer solution's penetration into the trenches, the silicon wafer was turned upside down and continuously mixed with the developer solution with a stirrer. In this way, the fresh developer solution could react with and remove the uncured photoresist. This step was followed by an ultrasonic bath where the remaining photoresist was removed. Once the silicon wafer mold was successfully generated, the standard replica molding process consisted of curing agent mixing, degassing, pouring, curing, peeling, punching, and plasma bonding for the fabrication of the final microfluidic device[20].

The functionality of the microfluidic device was experimentally determined by loading *Drosophila* embryos into the compression channels and applying positive pressure to the gas channels. Measurements of the decreasing width of the embryos under a microscope (**Figure 5A**) demonstrate how gas pressure can be used to obtain a target compression level (**Figure 5B**). Time-lapse images of aligned embryos undergoing compression also demonstrate this system's compatibility with confocal microscopy.

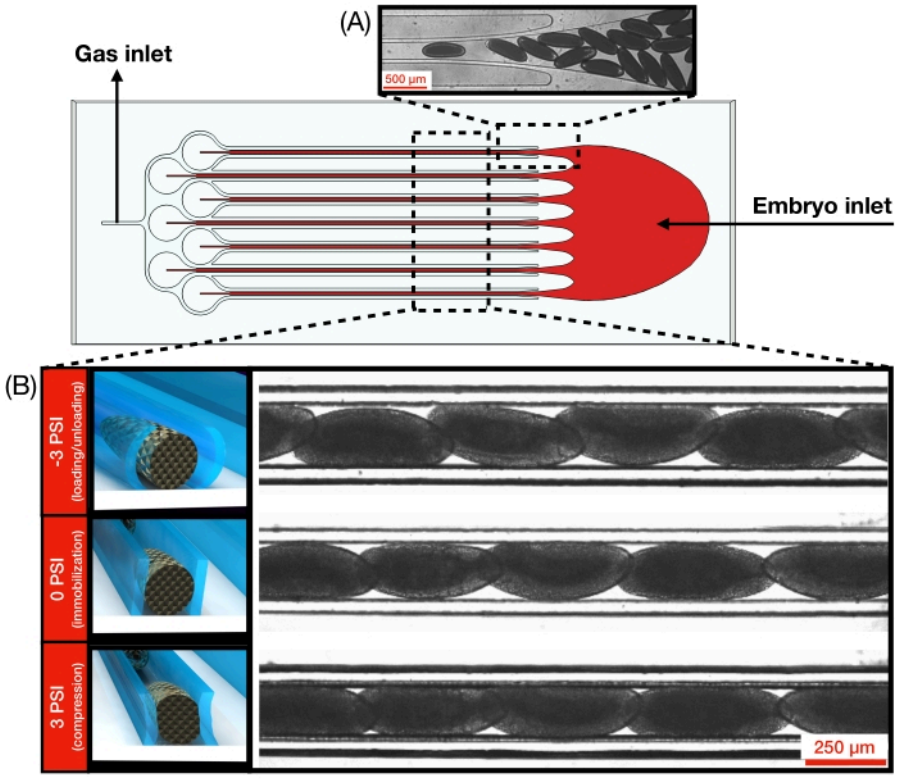

Figure 1: The design and function of the microfluidic device. The microfluidic device consists of seven parallel compression microchannels that can test up to 300 whole *Drosophila* embryos simultaneously. (**A**) Embryos were introduced into the device *via* the main embryo inlet, and they aligned along the posterior-anterior axis automatically as they entered the microchannels. (**B**) Embryos were freely moving when negative pressure was applied through the gas inlet as this deflected the deformable microchannel sidewalls outward. This allowed for their loading as well as unloading as a single lane. When the negative pressure was removed, the embryos were immobilized in the microchannels. When positive pressure was applied, the microchannel sidewalls compressed the embryos by deflecting inward. Please click here to view a larger version of this figure.

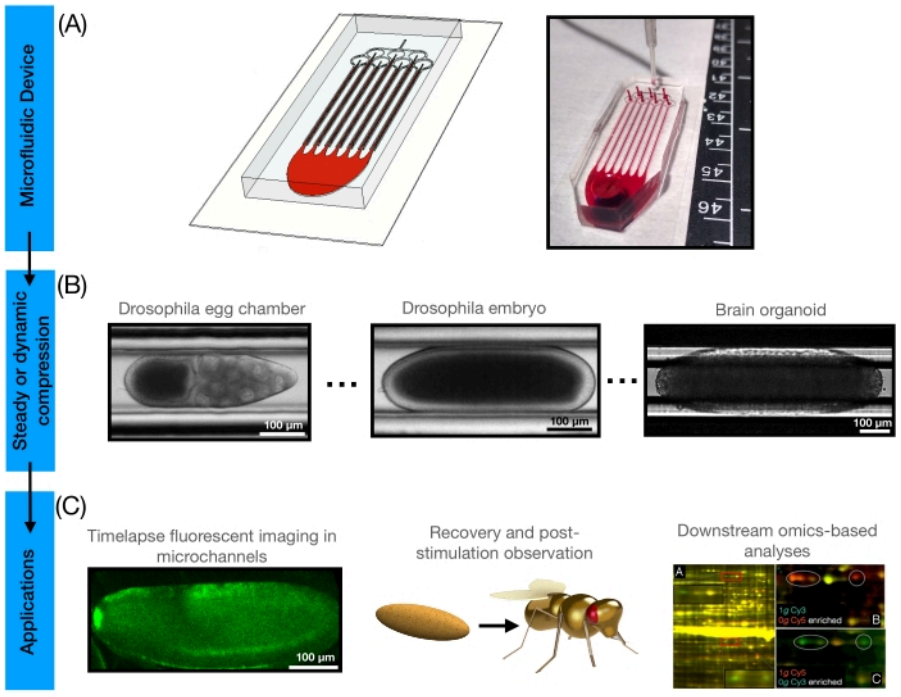

Figure 2: Process flow of microfluidic compression experiments for mechanobiology studies. (**A**) The high-throughput microfluidic mechanostimulation device is made of PDMS and a glass slide to process hundreds of multicellular biological samples. (**B**) The device is tailored to work with different multicellular systems such as *Drosophila* egg chambers, *Drosophila* embryos, or brain organoids. This device can apply steady or dynamic compression patterns to the biosystems. (**C**) The systems can be imaged with a confocal microscope over time as they are being compressed. The expression levels and localization of fluorescently labeled proteins in response to compression can be analyzed. Upon collection, the systems can be analyzed for post-stimulation testing and imaging. The high-throughput processing capability of the microfluidic device also allows the systems to be lysed and used in omics-based biological assays that require a large number of samples, as shown in the figure with a 2-dimensional differential gel electrophoresis image example. Please click here to view a larger version of this figure.

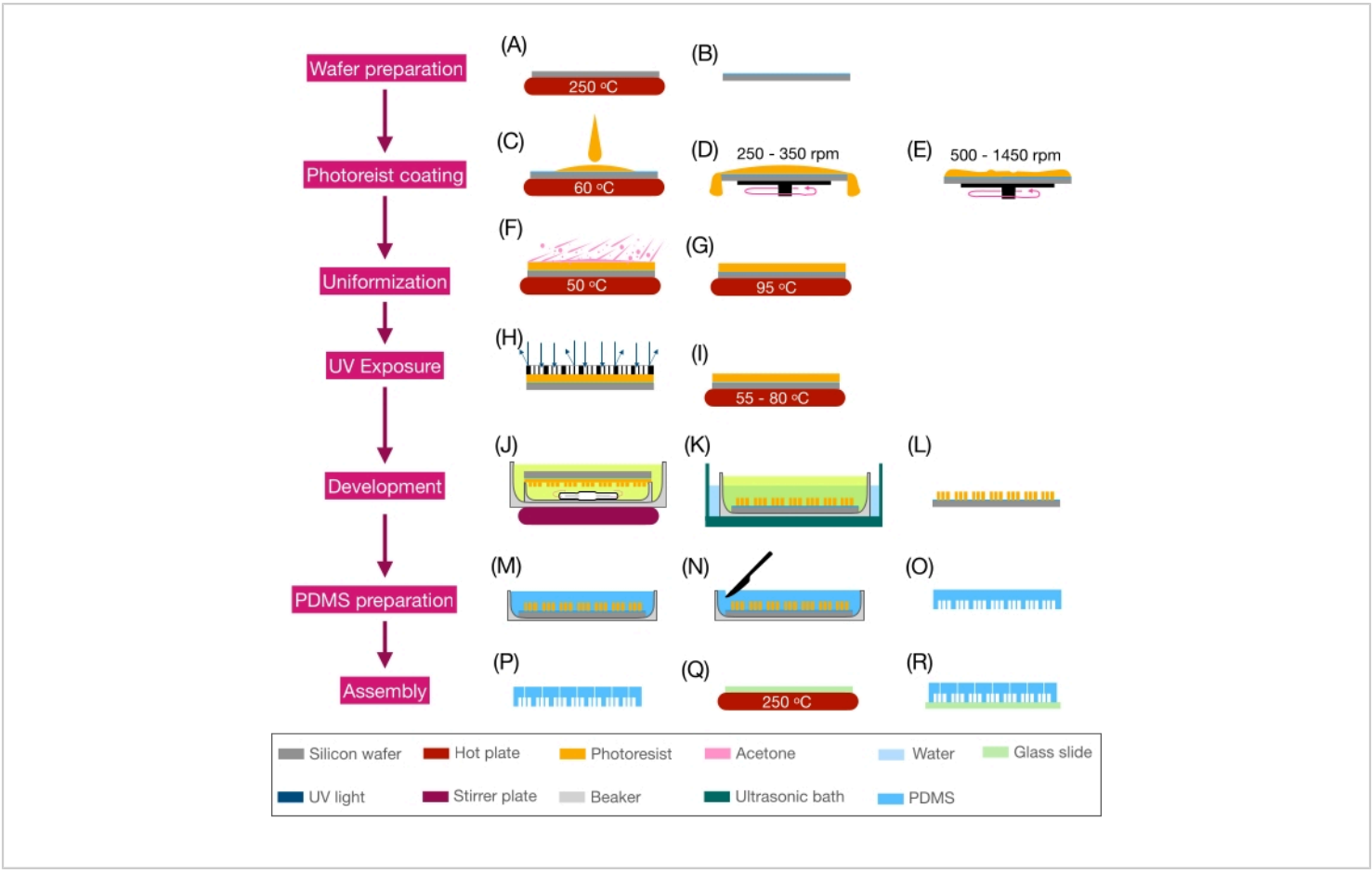

Figure 3: Fabrication process of the silicon wafer mold with thick photoresist and high aspect ratio trenches. (**A**,**B**) The overall fabrication process began with preparing the silicon wafer for photoresist coating. (**C**-**G**) A thick photoresist coating was uniformly applied to the silicon wafer. (**H**,**I**) The photoresist was patterned with UV exposure through the photomask. (**J**-**L**) Uncured photoresist was removed from the silicon wafer. (**M**-**P**) The PDMS part was fabricated through soft lithography. (**Q**,**R**) The device was sealed to the glass slide. Please click here to view a larger version of this figure.

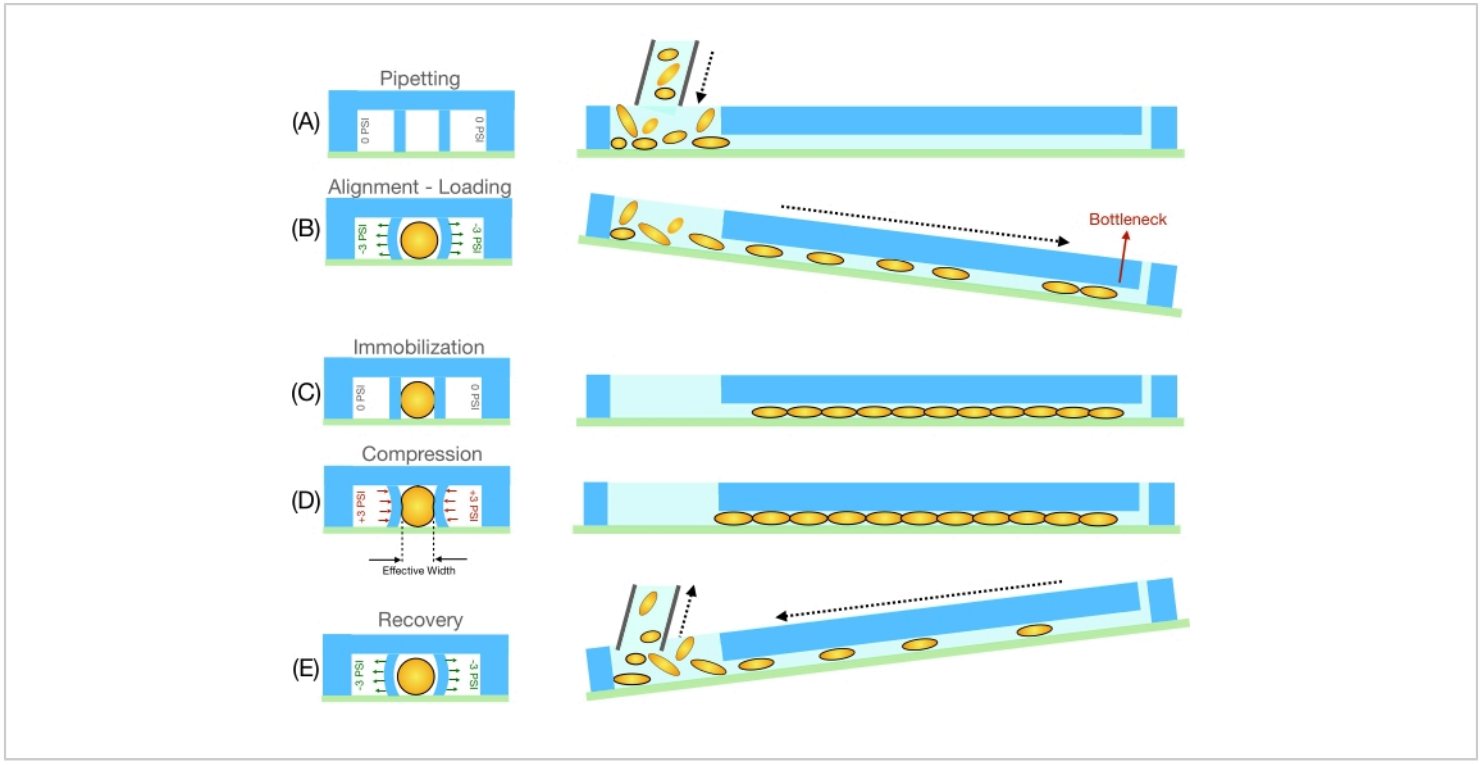

Figure 4: The operation of the microfluidic device. (**A**) First, embryos were pipetted into the main embryo inlet. (**B**) Second, negative pressure was applied to the gas inlet, and the microfluidic device was tilted downward to allow for the embryos to align and be loaded into the microchannels. (**C**) Third, negative pressure was removed to immobilize the embryos. (**D**) Fourth, positive pressure was applied to the gas channels to compress the embryos. (**E**) Lastly, the embryos were collected from the microfluidic device by switching back to negative pressure and tilting the microfluidic device upward. Please click here to view a larger version of this figure.

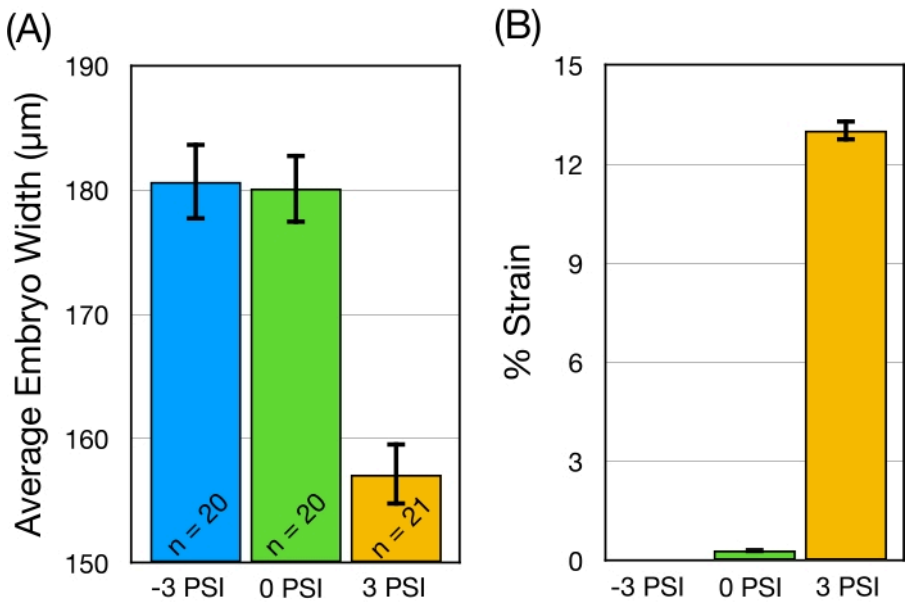

Figure 5: Experimental measurement of embryo compression level. (**A**) Representative embryos inside the microfluidic device under different gas pressure levels. While the embryos do not experience significant compression under vacuum or in neural pressure states, they are compressed when positive pressure is applied. (**B**) The amount of uniaxial compressive strain applied to the embryos at different gas pressure levels (error bars represent standard deviation). Please click here to view a larger version of this figure.

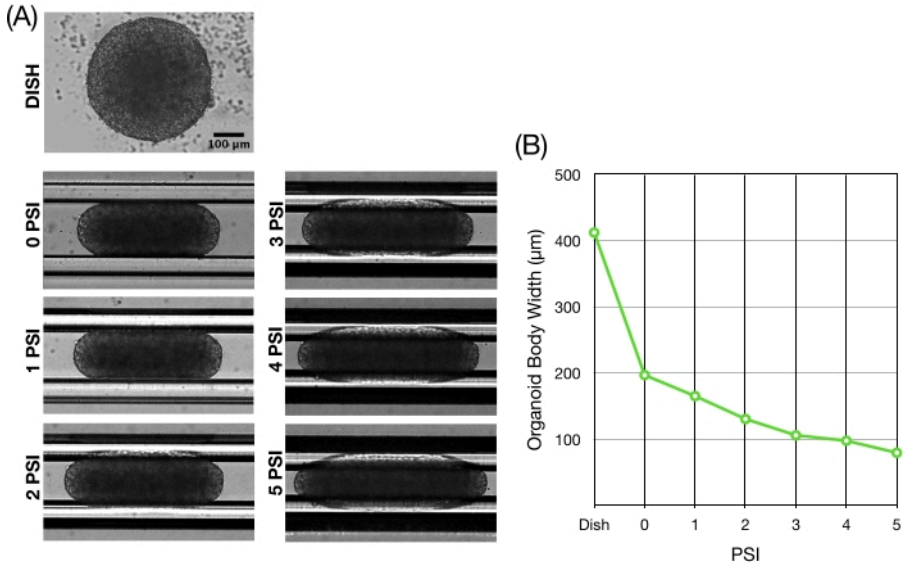

Figure 6: Compression of brain organoids in a microfluidic device designed and fabricated following the same strategy. (**A**) The compression of the brain organoids at increasing levels as the gas pressure is increased. (**B**) The width of the brain organoids inside the microchannels at different pressure levels. Please click here to view a larger version of this figure.

Supplementary Figure 1: Top view of the photomask used in the photolithographic fabrication of the silicon wafer mold. There are five identical microfluidic device geometries located within the 4 in diameter area. Please click here to download this File.

Supplementary Figure 2: Top view of the microfluidic device used in this study with the relevant dimensions. Please click here to download this File.

Discussion

The article describes the development of a microfluidic device to automatically align, immobilize, and precisely apply mechanical stimulation to hundreds of whole *Drosophila* embryos. The integration of the microfluidic system with a thin glass coverslip allowed for the imaging of embryos with high-resolution confocal microscopy during the stimulation. The microfluidic device also enabled the collection of the embryos right after the stimulation for running downstream biological assays. The design considerations, fabrication method, and characterization of this device were described in detail. The silicon wafer mold fabrication protocol allowed for the uniform thick coating of the photoresist with high aspect ratio trenches.

For this fabrication approach to be successful, it is important to lower the temperature of the baking steps and to minimize the heating and cooling rates of the silicon wafer after it is coated with photoresist. If this is not done properly, the photoresist coating can easily delaminate and alter the mold geometry. Once the silicon wafer mold is successfully fabricated, it can be copied into more durable materials to prevent damaging the original mold during consecutive

PDMS replica molding steps, which also contain heating and cooling cycles[21]. The fabrication of the PDMS microfluidic device through replica molding relies on the successful peeling of high aspect ratio sidewall structures from the mold. For this fabrication step to be reliable, it is critical to properly coat the surface of the silicon wafer with a silanizing agent to facilitate the peeling. The coating should also be renewed after fabricating approximately 20 PDMS devices to compensate for the partial removal of the silane layer during each peeling step. Otherwise, the sidewalls can become stuck inside the photoresist pattern, rendering the mold unusable. Since the level of compression applied to the samples is a function of the mechanical properties of the sidewalls, it is important to keep the PDMS replica molding process parameters consistent. The curing agent ratio, temperature, and duration must be closely monitored during fabrication. In addition, since this device strategy is for applying mechanical stimulation simultaneously to a large number of multicellular organisms, their aggregation inside the microchannels can lead to clogging. Although this problem was not experienced with the organisms utilized herein, if this does occur, there are potential solutions from the literature to overcome this problem, such as using carrier solutions during the introduction of the samples[22].

Although *Drosophila* embryos were used as a whole multicellular organism in this work, the design and fabrication strategy presented here can be applied to the mechanical stimulation of other multicellular systems by altering the device's dimensions accordingly (**Figure 2**). This can be accomplished by expanding the central microchannel width and height to match those of the multicellular systems. Through this approach, samples can enter the microchannels and be similarly compressed by deflecting the deformable sidewalls with positive pneumatic pressure. To demonstrate this approach, similar devices were fabricated for *Drosophila* egg chambers, as well as brain organoids. These systems enabled the precise mechanical compression of these biological systems similar to the *Drosophila* embryo experiments (**Figure 6**). Also, since this approach enables the replenishment of the media around the immobilized samples, it can be very useful for chemical stimulation experiments that require quick media exchange without disturbing the samples. Overall, this versatile approach combines the precision and high-throughput automation capabilities of microfluidic systems while enabling novel mechanobiology studies on various multicellular systems such as small tissue samples, organoids, embryos, and oocytes.

Disclosures

The authors have no financial interests in the products described in this manuscript and have nothing else to disclose.

Acknowledgments

This work was supported by the National Science Foundation (CMMI-1946456), the Air Force Office of Scientific Research (FA9550-18-1-0262), and the National Institute of Health (R01AG06100501A1; R21AR08105201A1).

References

1. Wang, J. H.-C., Thampatty, B. P. An introductory review of cell mechanobiology. *Biomechanics and Modeling in Mechanobiology.* **5** (1), 1-16 (2006).
2. Ingber, D. Mechanobiology and diseases of mechanotransduction. *Annals of Medicine.* **35** (8), 564-577 (2003).

3. Nims, R. J., Pferdehirt, L., Guilak, F. Mechanogenetics: Harnessing mechanobiology for cellular engineering. *Current Opinion in Biotechnology.* **73**, 374-379 (2022).
4. Bellin, R.M., et al. Defining the Role of Syndecan-4 in Mechanotransduction using Surface-Modification Approaches. *Proceedings of the National Academy of Sciences.* **106** 22102-22107 (2009).
5. Simpson, L. J., Reader, J. S., Tzima, E. Mechanical regulation of protein translation in the cardiovascular system. *Frontiers in Cell and Developmental Biology.* **8**, **34** (2020).
6. Humphrey, J. D., Schwartz, M. A. Vascular mechanobiology: Homeostasis, adaptation, and disease. *Annual Review of Biomedical Engineering.* **23**, 1-27 (2021).
7. Maurer, M., Lammerding, J. The driving force: Nuclear mechanotransduction in cellular function, fate, and disease. *Annual Review of Biomedical Engineering.* **21**, 443-468 (2019).
8. Jennings, B. H. *Drosophila*-A versatile model in biology & medicine. *Materials Today.* **14** (5), 190-195 (2011).
9. Konno, M. et al. State-of-the-art technology of model organisms for current human medicine. *Diagnostics.* **10** (6), 392 (2020).
10. Morgan, T. H. Sex limited inheritance in *Drosophila. Science.* **32** (812), 120-122 (1910).
11. Wu, Q., Kumar, N., Velagala, V., Zartman, J. J. Tools to reverse-engineer multicellular systems: Case studies using the fruit fly. *Journal of Biological Engineering.* **13** (1), 1-16 (2019).
12. Jayamohan, H. et al. Chapter 11 - Advances in Microfluidics and Lab-on-a-Chip Technologies. In *Molecular Diagnostics,* .edited by Patrinos, G., 197-217. Academic Press. Cambridge, MA (2017).
13. Scheler, O., Postek, W., Garstecki, P. Recent developments of microfluidics as a tool for biotechnology and microbiology. *Current Opinion in Biotechnology.* **55**, 60-67 (2019).
14. Mohammed, D. et al. Innovative tools for mechanobiology: Unraveling outside-in and inside-out mechanotransduction. *Frontiers in Bioengineering and Biotechnology.* **7**, 162 (2019).
15. Shorr, A. Z., Sönmez, U. M., Minden, J. S., LeDuc, P. R. High-throughput mechanotransduction in *Drosophila* embryos with mesofluidics. *Lab on a Chip.* **19** (7), 1141-1152 (2019).
16. Kim, Y.T., et al. Mechanochemical Actuators of Embryonic Epithelial Contractility. *Proceedings of the National Academy of Sciences.* **111**(40), 14366-14371 (2014).
17. Ashburner, M. *Drosophila. A Laboratory Handbook.* Cold Spring Harbor Laboratory Press. Long Island, NY. (1989).
18. Qin, D., Xia, Y., Whitesides, G. M. Soft lithography for micro-and nanoscale patterning. *Nature Protocols.* **5** (3), 491 (2010).
19. Lee, H. et al. A new fabrication process for uniform SU-8 thick photoresist structures by simultaneously removing edge bead and air bubbles. *Journal of Micromechanics and Microengineering.* **21** (12), 125006 (2011).
20. Xia, Y., Whitesides, G. M. Soft lithography. *Annual Review of Materials Science.* **28** (1), 153-184 (1998).

21. Sonmez, U. M., Coyle, S., Taylor, R. E., LeDuc, P. R. Polycarbonate heat molding for soft lithography. *Small.* **16** (16), 2000241 (2020).

22. Levario, T. J., Zhan, M., Lim, B., Shvartsman, S. Y., Lu, H. Microfluidic trap array for massively parallel imaging of *Drosophila* embryos. *Nature Protocols.* **8** (4), 721-736 (2013).